Int. J. Heat Mass Transfer. Vol. 20, pp. 1339–1350. Pergamon Press 1977. Printed in Great Britain

TURBULENT MASS TRANSFER WITH A FIRST-ORDER CHEMICAL REACTION ON A WALL AT $Pr \gg 1$

B. A. KADER and A. A. GUKHMAN
Moscow Institute of Mechanical Engineering for Chemical Industry,
Moscow, U.S.S.R.

(*Received* 26 *November* 1975)

Abstract—Mass transfer between a turbulent fluid flow and a flat smooth wall with a first-order chemical reaction on it has been investigated. An extreme case of an infinitely high reaction rate (constant concentration of passive admixture on the wall) has been analysed.

Three possible cases are considered consecutively. For very short plates which cannot be described by the boundary-layer approximation, a computer solution has been obtained by the finite difference method. This solution completely allows for both the edge (longitudinal molecular diffusion of a passive admixture) and surface (finite rate of a chemical reaction) effects which are rather essential for small-length plates. For those plates which can be interpreted by the boundary-layer approximation with the neglect of the effect of turbulent mass transfer, the analytical solution to the problem has been derived. The numerical data are compared with those obtained by the method of the equally accessible surface and in the boundary-layer approximation. As a result, the lower region limit of the plate sizes can be established where the edge effects may be neglected. These results may be directly applied to the theory of electrodiffusional and thermal (with coatings) small-size film sensors, designed for measuring local characteristics of friction, and heat and mass transfer to a smooth solid wall in a fluid flow.

Considering long plates for which turbulent mass transfer is of importance, a simple approximate solution of the problem is obtained. The numerical parameters involved in this solution are thus chosen to fit the asymptotic results obtained close to the leading edge of the plate and far from it. These results make it possible to determine the mass-transfer entry region in the arbitrary cross section channel and to suggest simple formulae for calculating the local and channel length-averaged mass transfer intensity in the entry region. These formulae are checked by the reported experimental data.

NOMENCLATURE

A, $= \dfrac{\Gamma(1/3)}{\sqrt[3]{3}\Gamma(2/3)} \dfrac{k}{u_*} l_+^{1/3} Pr^{2/3} = \dfrac{\Gamma(1/3)}{\sqrt[3]{3}\Gamma(2/3)} KL^{1/3}$;

a, thermal diffusivity;

B, $= \left(1 + \dfrac{2\pi}{\sqrt[3]{3}} \dfrac{G}{\sqrt[3]{b}}\right)^{-1}$;

b_{ij}, first coefficient of the Taylor expansion of K_{ij};

b, first coefficient of the Taylor expansion of K_{yy};

c, passive admixture concentration;

C, $= 9bl_+$;

d, tube diameter;

D, molecular diffusivity;

F, Green function of equation (6);

G, $= \dfrac{k}{u_*} Pr^{2/3}$;

h, plate width;

J_w, $= \dfrac{\sqrt{vD}}{c_0 u_*} \dfrac{\partial \bar{c}}{\partial y}(x, 0)$, local mass flux on the plate surface;

K, $= k/u_* \sqrt{Pr}$;

K_{ij}, tensor components of eddy diffusivity;

k, surface reaction rate;

l, plate length or equivalent channel diameter;

l_s, stabilization length for Nu;

L, $= l_+ \sqrt{Pr} = lu_*/\sqrt{vD}$;

L_s, stabilization length for $\langle Nu \rangle$;

n_{ij}, exponent at the first term of the Taylor expansion of K_{ij} with the factor b_{ij} different from zero;

n, exponent at the first term of the Taylor expansion of K_{yy};

r_*, chosen accuracy [%];

S, $= J_w L^{1/3}$, normalized concentration gradient at the plate surface;

u, velocity at the point considered;

u_*, $= \sqrt{\tau_w/\rho}$, friction velocity;

u_x, u_y, instantaneous components of the velocity vector in x- and y-directions;

x, longitudinal coordinate relative to the leading edge;

X, $= \dfrac{xu_*}{\sqrt{vD}}$, dimensionless longitudinal coordinate;

y, normal-to-the-wall coordinate;

Y, $= \left(\frac{L^2}{9}\frac{l}{x}\right)^{1/3}\frac{y}{l}$,
dimensionless normal-to-the wall coordinate;
z, $= y_+/\delta(x)$;
α, $= \left(\frac{9}{L^2}\frac{x}{l}\right)^{1/3}$;
β, γ, dimensionless quantities defined by formula (40);
Γ, Euler' gamma-function;
$\delta(x)$, concentrational boundary-layer thickness;
θ, $= \frac{c_0 - \bar{c}}{c_0}$, dimensionless concentration;
μ, dynamic viscosity;
ν, kinematic viscosity;
ξ, $= \frac{x}{l}$, dimensionless longitudinal coordinate;
ρ, density;
τ_w, wall shear stress;
ϕ, confluent hypergeometric function;
ω, constant defined by formula (43);
Nu, $= \frac{j_w l}{c_0 D}$, Nusselt number;
Pr, $= \nu/D$, Prandtl number;
Re, ul/ν, Reynolds number.

Subscripts and superscripts

$'$, fluctuation (the difference between the instantaneous quantity and its corresponding mathematical expectation);
w, wall conditions;
$-$, mathematical expectation;
$\langle\ \rangle$, length averaging;
∞, stabilized conditions;
$+$, quantity dimensionalized by the wall parameters u_* and ν;
0, infinity conditions.

1. STATEMENT OF THE PROBLEM

CONSIDER a rectangular plate h wide in the field of uniform shear stresses. Let the plate length in the flow direction be $l \ll h$, so that the edge effects in the direction perpendicular to the flow can be neglected. Assume that in a fluid flow around the sensor there is a uniformly distributed passive (i.e. not affecting the flow dynamics) admixture. The x-axis is along the flow, while y is normal to the wall. Then, the steady-state diffusion equation is of the form

$$\bar{u}(y)\frac{\partial \bar{c}}{\partial x} = D\left(\frac{\partial^2 \bar{c}}{\partial x^2} + \frac{\partial 2\bar{c}}{\partial y^2}\right) - \frac{\partial}{\partial x}(\overline{u_x' c'}) - \frac{\partial}{\partial y}(\overline{u_y' c'}) \quad (1)$$

where primes indicate fluctuations, i.e. the difference between the instantaneous and their corresponding mean values. The concentration of a passive admixture $c(x, y)$ at a large distance from the plate is constant

$$\bar{c}(x, \infty) = c_0; \quad \bar{c}(-\infty, y) = c_0 \quad (2)$$

and on the plate surface the first-order reaction takes place

$$D\frac{\partial \bar{c}}{\partial y}(x, 0) = \begin{cases} 0 & \text{at } x < 0 \text{ or } x > l \\ k\bar{c}(x, 0) & \text{at } 0 \leqslant x \leqslant l. \end{cases} \quad (3)$$

At large values of the reaction rate constant ($k \to \infty$), the latter equation transforms into an ordinary boundary condition for the constant wall concentration $\bar{c}(0 \leqslant x \leqslant l, 0) = c_w$. At $Pr \gg 1$, the resistance to mass transfer is completely due to the viscous sublayer of the turbulent boundary layer, for which the velocity distribution can be approximated by the linear function

$$\bar{u}(y) = yu_*^2/\nu. \quad (4)$$

Equation (1) with boundary conditions (2) and (3) describes a broad range of problems which are important not only for chemical engineering but also for the theory of film (thermal† and electrodiffusional) sensors being nowadays widely used in practice. For the thermal film element, k entering into equation (3) represents thermal resistance of the insulating coating of the heated film which is an unseparable part of the sensor when used in fluid flows. For the electrodiffusional sensor, the constant k is the rate of the electrochemical reaction of working ions on the sensor surface. Here, the effective value of k may also show an existing state of the sensor surface. The use of bulky installations with a large amount of electrolyte employed for several days (sometimes even weeks) prohibits such cleaning of the sensor surface that allows necessary calculations relied only on the kinetic laws of electrochemical reaction and the laws governing ion transfer through the sensor boundary layer. One can suppose that because of incomplete cleaning of the sensor, a uniform layer exerting constant resistance to mass transfer is formed on its surface. An ion flux through such a layer is proportional to the difference of concentrations at both boundaries of this layer. It is readily seen that this extra resistance effect can be easily allowed for by introducing a certain fictitious rate of the electrochemical reaction different from the one characteristic of purely diffusional overstress conditions. Later on, for the sake of clarity, we shall speak of the electrochemical diffusional sensor, for the operational principles of the diffusional sensor and constant-temperature thermal film element are practically identical.

† Further arguments are only true of the thermal film element of such a small extent in the flow direction that the thickness of the thermal layer formed on its surface does not exceed that of the viscous sublayer of the turbulent boundary layer (i.e. of the sublayer where the velocity distribution obeys equation (4) with sufficient accuracy). It should be added that the heat is considered here to be passive admixture (i.e. only low-intensity heat fluxes are analysed). It is supposed, as usual, that the mechanism of turbulent heat transfer is exactly the same as that of passive admixture.

For the last two decades, the theory of these sensors has been extensively developed by German [1, 2], American [3–7], Soviet [8–10], French [11] and Japanese [12, 13] scientists. However, in nearly all of these works the diffusional sensor theory is studied in the frame of the boundary-layer approximation, and the rate of the appropriate electrochemical reaction is considered infinitely great.

In respect of such a statement of the problem, the following remarks can be made. The sensors of small extent in the direction of the averaged flow, most of all, satisfy the aims of local measurements of the boundary-layer characteristics. Still more important is the reduction in the size of the sensor designed for determining the fluctuation characteristics of the boundary layer, when the sensitivity of a measuring element decreases sharply with the increase of its size [9]. It is known, meanwhile, that the boundary-layer approximation is too crude for the study of a real concentration distribution near the sensor edges, i.e. in the region of a sharp change in wall conditions, where the molecular diffusion in the directions parallel to the wall may bring about an appreciable error in the calculations based on this approximation. This extent of the error is most significant for small-size sensors.

To the above remarks the following should be added. As the electrode surface is not equally accessible and the reaction rate is finite, the concentration of reacting charged particles on the sensor edge surfaces ranges from the initial value to zero; that is, some portion of the electrode is not polarized. Since the effect of the finite reaction rate is also most pronounced near the diffusion sensor edges, these two effects should be considered jointly.

In the literature available, the estimates were made only of the above effects taken separately. The numerical analysis of the edge effects for the small-size completely polarized sensors was performed by Ling [4], while the concentration distribution along the sensor surface was investigated within the framework of the boundary-layer approximation in [2, 10]. Neither of these effects was regarded at all in analytical studies of the sensitivity of the electrochemical sensor to the fluctuations in the viscous sublayer of the turbulent boundary layer [7, 9–11, 13].

We shall therefore make first a detailed consideration of steady-state mass transfer between a turbulent fluid flow and a small-size plate with the first-order chemical reaction on the wall. In this case, because of the edge effects, the boundary-layer approximation is not applicable (one cannot assume that $\partial^2\bar{c}/\partial x^2 = 0$) but, on the other hand, the layer of diffusional disturbance produced by the plate is so thin that the effect of turbulence in the viscous sublayer can be neglected.

$$[\partial\overline{(u_x'c')}/\partial x = 0 \text{ and } \partial\overline{(u_y'c')}/\partial y = 0].$$

All the results obtained with this assumption may be naturally applied to a laminar flow.

Then we examine long plates, for which the effect of turbulent fluctuations in the viscous sublayer of the turbulent boundary layer starts to show itself appreciably in the bulk of the flux to their surfaces, but the edge effects are negligible.

2. CONCENTRATION FIELD AND MASS FLUX TO A SHORT PLATE

In the conditions considered, the concentration field near the plate is determined by the equation

$$\frac{u_*^2}{\nu} y \frac{\partial\bar{c}}{\partial x} = D\left(\frac{\partial^2\bar{c}}{\partial x^2} + \frac{\partial^2\bar{c}}{\partial y^2}\right) \tag{5}$$

with boundary conditions (2) and (3).

The problem has been solved on the computer by the successive iteration method applied earlier by Ling [4] for $k = \infty$. The range of $5 \leqslant L \leqslant \sqrt{5000}$ and $0.01 \leqslant k \leqslant \infty$ is analysed. The numerical results are given in Figs. 1–4 and Table 1.

The lines given in Fig. 1 represent constant concentration in the vicinity of plates of constant dimensionless length ($L = \sqrt{50}$) calculated at different dimensionless rates of a surface reaction $0.01 \leqslant k \leqslant \infty$. The boundary of the diffusional layer $\theta = 0.01$ is also shown in this figure. It is clear that the thickness of the thermal boundary layer is finite at the leading edge. However, the effect of the longitudinal molecular diffusion provoking a change in concentration before the plate becomes less significant with the decrease of k. Behind the plate, a significant "diffusional wake" is

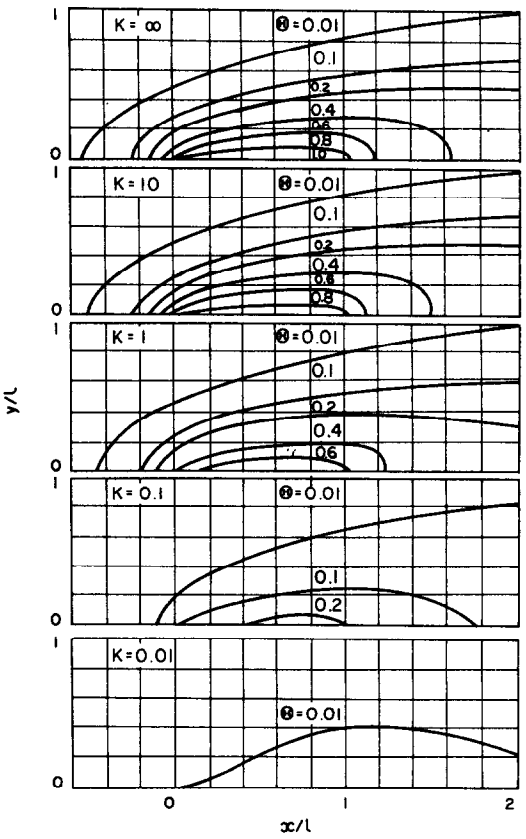

FIG. 1. Concentration field close to a short plate ($L = \sqrt{50}$) at different dimensionless rates of surface reaction K.

observed which may cause introduction of important corrections into the correlation measurements performed with film sensors [12]. It is worth noting that even at large relative rate of a surface reaction, $k = 10$, the electrodiffusional sensor is incompletely polarized ($\theta_w \neq 1$) over its length. This situation is illustrated in Fig. 2 plotting the distribution of dimensionless surface

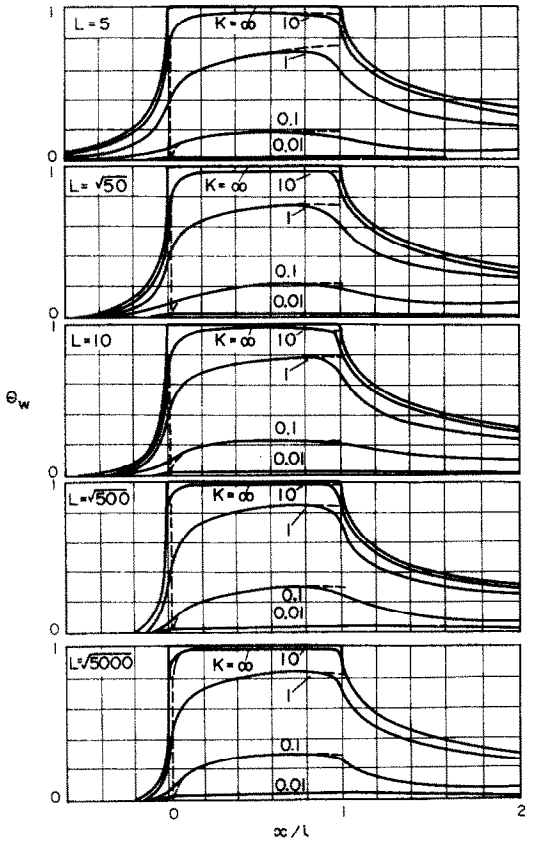

FIG. 2. Distribution of wall concentration over the plates of different length. Solid lines, numerical results; dashed lines, calculations in the boundary-layer approximation.

concentration over the different-size plates, $5 \leqslant L \leqslant \sqrt{5000}$, and at various reaction rates, $0.01 \leqslant k \leqslant \infty$. One can readily see from these plots that polarization of the electrodiffusional sensor increases with its length and k, which agrees with the existing idea that the importance of the edge effects should fall as fast as the length of film sensors increases. The concentration field close to the centre of a fairly large plate is believed to be well determined by the boundary-layer approximation

$$\frac{u_*^2}{\nu} y \frac{\partial \bar{c}}{\partial x} = D \frac{\partial^2 \bar{c}}{\partial y^2} \tag{6}$$

at boundary conditions

$$\bar{c}(x, \infty) = c_0; \quad \bar{c}(0, y) = c_0;$$

$$D \frac{\partial \bar{c}}{\partial y}(x > 0, 0) = k\bar{c}(x > 0, 0). \tag{7}$$

Define the Green function $F(x, y, \xi)$ of differential equation (6) by solving it under the boundary conditions with a single surface concentration jump at the point $\xi = x$

$$c_w(x) = \begin{cases} 1 & \text{at} \quad 0 < x < \xi \\ 0 & \text{at} \quad \xi < x < l \end{cases} \tag{8}$$

and $c(x, \infty) = 1$.

It is evident that in this case

$$F(x, y, \xi) = \begin{cases} \dfrac{1}{\Gamma(4/3)} \displaystyle\int_0^{y\sqrt[3]{\frac{g\mu D}{\tau_w}(x-\xi)}} e^{-\zeta^3} d\zeta & \\ & \text{at} \quad \xi < x < l \\ 1 & \\ & \text{at} \quad 0 < x < \xi. \end{cases} \tag{9}$$

Using the superposition principle for approximating an arbitrary distribution function, $c_w(x)$, we can represent the concentration field, $c(x, y)$, in the vicinity of the sensor as the Duhamel integral

$$c(x, y) = \int_0^l F(x, y, \xi) \, dc_w(\xi), \tag{10}$$

where the integral equation for the ion concentration distribution on the electrode surface under the conditions considered will be of the form [14, 15]

$$kc_w(x) \frac{\Gamma(4/3)}{D} (g\mu D)^{1/3} / \tau_w^{1/3} = -\int_0^x \frac{dc_w/d\xi}{(x-\xi)^{1/3}} d\xi. \tag{11}$$

An approximate solution to equation (11) is given in [10]. The second-kind Volterra integral equation can be exactly solved by the Laplace transformation. It can be conveniently expressed in terms of the confluent hypergeometric functions

$$\theta_w(\xi) = \sum_{m=1}^{\infty} \frac{(-1)^{m+1}}{\Gamma\left(\dfrac{m+3}{3}\right)} (A\xi^{1/3})^m$$

$$= 1 - \exp(-A^3\xi) + \frac{(A^3\xi)^{1/3}}{\Gamma(4/3)} \times \phi(1, \tfrac{4}{3}; -A^3\xi)$$

$$- \frac{(A^3\xi)^{2/3}}{\Gamma(5/3)} \phi(1, \tfrac{5}{3}; -A^3\xi). \tag{12}$$

Hence the sensor length-averaged surface concentration can be easily found

$$\langle \theta_w \rangle = 1 + \frac{\exp(-A^3) - 1}{A^3} + \frac{A}{\Gamma(7/3)} \phi(1, \tfrac{7}{3}; -A^3)$$

$$- \frac{A^2}{\Gamma(8/3)} \phi(1, \tfrac{8}{3}; -A^3). \tag{13}$$

The expressions obtained are convenient to estimate the asymptotic behaviour of the solution at $A^3\xi \gg 1$ and $A^3\xi \ll 1$ but are of little use for $A^3\xi \sim 1$. At $A^3\xi \sim 1$, the approximate method of the equally accessible

Table 1. Comparison of the results obtained (a) by the computer; (b) by the boundary-layer approximation; (c) by the method of equally accessible surface

K		L = 5		L = √50		L = 10		L = √500		L = √5000	
		⟨θ_w⟩	⟨S⟩	⟨θ_w⟩	⟨S⟩	⟨θ_w⟩	⟨S⟩	⟨θ_w⟩	⟨S⟩	⟨θ_w⟩	⟨S⟩
	a	1.000	0.893	1.000	0.871	1.000	0.852	1.000	0.820	1.000	0.809
	b	1.000	0.807	1.000	0.807	1.000	0.807	1.000	0.807	1.000	0.807
	c	1.000	0.807	1.000	0.807	1.000	0.807	1.000	0.807	1.000	0.807
	a	0.949	0.852	0.955	0.832	0.961	0.816	0.971	0.799	0.981	0.793
10	b	0.955	0.773	0.960	0.777	0.964	0.781	0.972	0.787	0.981	0.793
	c	0.955	0.762	0.960	0.768	0.964	0.772	0.972	0.779	0.981	0.787
	a	0.661	0.572	0.690	0.594	0.713	0.613	0.769	0.643	0.834	0.680
1	b	0.690	0.529	0.711	0.555	0.732	0.578	0.778	0.627	0.836	0.680
	c	0.691	0.527	0.715	0.547	0.737	0.566	0.785	0.607	0.841	0.656
	a	0.159	0.143	0.178	0.157	0.199	0.172	0.246	0.211	0.327	0.277
0.1	b	0.164	0.143	0.183	0.157	0.201	0.172	0.248	0.212	0.327	0.278
	c	0.190	0.139	0.203	0.152	0.228	0.166	0.278	0.204	0.369	0.276
	a	0.0185	0.0167	0.0211	0.0187	0.0243	0.0207	0.0321	0.0272	0.0456	0.0393
0.01	b	0.0193	0.0168	0.0217	0.0188	0.0243	0.0210	0.0315	0.0273	0.0456	0.0395
	c	0.0232	0.0167	0.0260	0.0187	0.0291	0.0209	0.0377	0.0272	0.0543	0.0391

surface [15] may be used, that gives

$$\theta_w = \frac{\Gamma(2/3)A\xi^{1/3}}{1+\Gamma(2/3)A\xi^{1/3}}, \tag{14}$$

$$\langle\theta_w\rangle = 1 - \frac{3}{2A\Gamma(2/3)} + \frac{3}{A^2\Gamma^2(2/3)} - \frac{3}{A^3\Gamma^3(2/3)}\ln[1+A\Gamma(2/3)]. \tag{15}$$

In Fig. 2 the dotted line shows the calculation results by formula (12). As one should expect, this solution describes poorly the real concentration field in the immediate vicinity of the leading and trailing edges, but agrees well with the numerical calculation for the middle area. As follows from the general boundary-layer theory, the width of this area increases with the plate length. It is worth noting that the existing difference between the analytical and numerical solutions, i.e. smaller predicted values of θ_w at the leading edge and larger ones at the trailing edge, makes it possible to assume that the plate length-averaged $\langle\theta_w\rangle$ obtained from an exact calculation and in the boundary-layer approximation should not severely differ even for relatively short sensors. Table 1 shows that this is really true: even for the shortest plates ($L = 5$), the difference does not exceed 8%.

The longitudinal molecular diffusion has a more essential effect on the surface concentration gradients.

As follows from Leveque's solution [16], the boundary-layer thickness at the leading edge is zero and the concentration gradient is then governed by

$$J_w(X) = \frac{\sqrt{vD}}{c_0 u_*}\frac{\partial\bar{c}}{\partial y}(x>0, 0) = \frac{\sqrt[3]{3}}{\Gamma(1/3)}X^{-1/3}, \tag{16}$$

tends to infinity at $X \to 0$ and decreases monotonically with increasing X. The numerical results giving a real picture of a normalized concentration gradient distribution along the sensor length are presented in Fig. 3 where the dotted line shows the results obtained by the boundary-layer approximation.

The computer calculations (Fig. 4) indicate that at the leading edge of the plate, the concentration

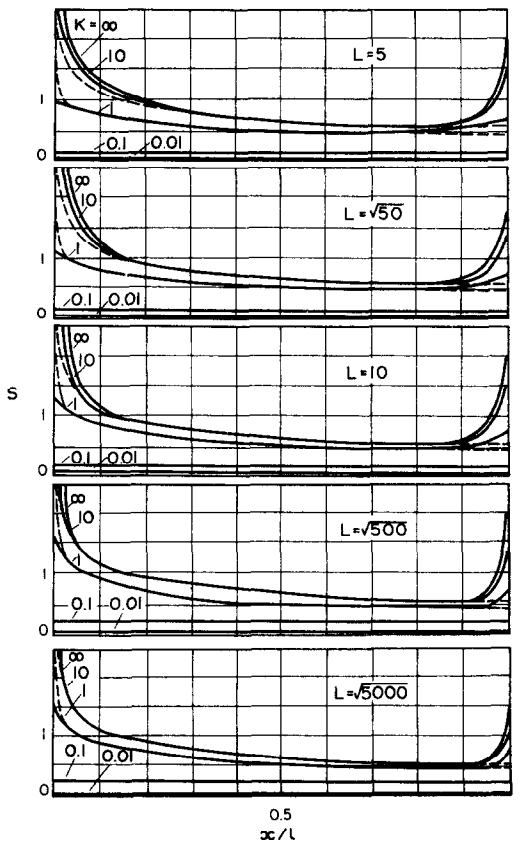

FIG. 3. Distribution of dimensionless wall concentration gradients over the plates of different length. Solid lines, numerical results; dashed lines, calculations in the boundary-layer approximation.

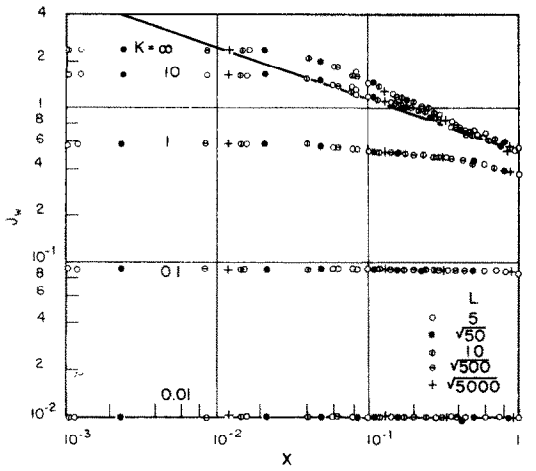

FIG. 4. Dimensionless mass flow close to the leading edge of the plate. Solid line, calculation in the boundary-layer approximation.

gradient assumes a constant value which depends on the rate of a chemical reaction. For the finite K, this follows directly from boundary condition (3). Unlike equation (16), at $K = \infty$, in accordance with the numerical calculation for $xu_*/\sqrt{\nu D} < 0.02$, we have

$$\frac{\sqrt{\nu D}}{c_0 u_*}\frac{\partial \bar{c}}{\partial y}(x,0) = 2.40.\dagger \qquad (17)$$

Such a difference does not affect the total mass flux appreciably but is of importance for the theory of film sensor measurements of the boundary-layer fluctuation structure. There is good reason to believe that the structure of the concentration field near the leading edge (being here of the smallest thickness and, hence, of the smallest persistence) affects decisively the sensor characteristics in the high-frequency region.

An increase in the concentration gradients near the trailing edge of the sensor is of greater significance. Following the boundary-layer approximation, at finite K for the normalized concentration gradient on the plate surface, we have

$$S = L^{1/3}J_w = L^{1/3}K(1-\theta_w). \qquad (18)$$

At low K, a short electrodiffusional sensor is not practically polarized at all ($\theta_w \sim 0$), so that $S = L^{1/3}K$, and does not change along the plate. In this case, the integral mean $\langle S\rangle$

$$\langle S\rangle = L^{-2/3}\int_0^L J_w(X)\,dX = L^{1/3}K(1-\langle\theta_w\rangle) \qquad (19)$$

is very accurately described not only by the boundary-layer approximation but also by the method of the equally accessible surface even for short plates. This should not be astonishing if you remember the above situation of decreasing longitudinal concentration gradients with K and the contribution of longitudinal molecular diffusion. Also note that at $K \leqslant 1$, the theoretical results for the leading edge region lie above the computer data, while the picture is reverse for the trailing edge region. One can therefore suppose that the sensor integral means should not differ considerably. The data summarized in Table 1 support this idea. For $K \geqslant 10$, the deviations (neglecting the regions of $X < 10^{-3}$) are of a constant sign, and the difference in the results becomes more noticeable. At $K \to \infty$, we have the equation $\langle S\rangle = \sqrt[3]{3}/2\Gamma(4/3) = 0.807$, by virtue of formula (16).

For estimation of the appropriate correction for the normalized dimensionless surface concentration gradient, S_T, predicted by the boundary-layer theory, the approximation equation

$$\langle S\rangle = \langle S_T\rangle + \frac{0.43}{L}\exp\left(-\frac{3}{4K}\right) \qquad (20)$$

can be used.

For $K \leqslant 0.1$, the correction is insignificant at any practically interesting L. The accuracy of the approximation suggested is 2% in the whole range of L and K.

The local and integral dimensionless mass-transfer coefficients on a short plate can be easily estimated by the value of the normalized surface concentration gradient

$$Nu = SL^{2/3}, \quad \langle Nu\rangle = \langle S\rangle L^{2/3}. \qquad (21)$$

3. MASS TRANSFER TO A LONG PLATE

Considering long plates, we should treat incomplete equation (1), provided that $\partial^2\bar{c}/\partial x^2 = 0$, because in this case the edge effects of molecular conductivity should not, as is shown above, play any role. To solve the equation derived, different ways of its closing are used, the simplest of which, assuming a linear relationship between the turbulent admixture flux and mean concentration gradient of admixture $\overline{u'_x c'}$, $\overline{u'_y c'}$, goes far back to Boussinesq [20]. In a general anisotropic case, this assumption is of the form

$$\overline{u'_x c'} = -K_{xx}\frac{\partial \bar{c}}{\partial x} - K_{xy}\frac{\partial \bar{c}}{\partial y},$$

$$\overline{u'_y c'} = -K_{yx}\frac{\partial \bar{c}}{\partial x} - K_{yy}\frac{\partial \bar{c}}{\partial y}, \qquad (22)$$

where the eddy diffusivity tensor coefficients (K_{ij}) depend, in general, on the x,y-coordinates. In the majority of the published works using this approach, it is supposed (usually without any grounds) that x, y are the major axes of the tensor K_{ij}, i.e. $K_{xy} = 0$, $K_{yx} = 0$. Here either $K_{xx} = 0$ is assumed or the estimate of $K_{xx} = K_{yy}$ is introduced. The assumption on the diagonal nature of the turbulent diffusivity tensor relies on the situation that the directions of the axes are determined by the conditions of a hydrodynamically stabilized tube flow. This argument, however, is not strict [21]. Indeed, in line with [21], we may show, for example, that the longitudinal component of turbulent mass transfer due to the transverse concentration gradient is different from zero (i.e. $K_{xy} \neq 0$).

† The latter result is inconsistent with the results of some recent analytical studies [17, 18]. The reasons for such a deviation are analysed in detail in [19].

Let us now assume that the components of the tensor K_{ij} depend only on the radial position and do not depend on the longitudinal coordinate. This hypothesis can be maintained by a decisive role of flow dynamics, which in this case is believed to be completely stabilized, so that the tensor components of the eddy momentum diffusivity (i.e. eddy viscosity tensor) are independent of x. In the depth of the viscous sublayer of the turbulent boundary layer, where the total resistance to mass transfer is concentrated at $Pr \gg 1$, the tensor components of the eddy diffusivity are described, with appropriate accuracy, by their first terms of the corresponding Taylor power expansion

$$K_{ij} = \nu b_{ij}\left(\frac{yu_*}{\nu}\right)^{n_{ij}}. \tag{23}$$

Using the continuity equation, we can show that n_{yx} and $n_{yy} \geqslant 3$, while n_{xx} and $n_{xy} \geqslant 2$. The value of $n_{yy} = n$ seems to be of special importance. Based on the analysis suggested in [22], assume that $n = 3$.

In view of the above, equation (1), when expressed in terms of the dimensionless variables of the boundary-layer theory,

$$\theta = \frac{c_0 - \bar{c}}{c_0},\quad \xi = \frac{x}{l},\quad Y = \left(\frac{L^2}{9}\frac{l}{x}\right)^{1/3}\frac{y}{l} = \frac{1}{\alpha}\frac{y}{l} \tag{24}$$

takes the form

$$\begin{aligned}(1+C\xi Y^3)\frac{\partial^2\theta}{\partial Y^2} + 3Y^2(1+C\xi)\frac{\partial\theta}{\partial Y} - 9\xi Y\frac{\partial\theta}{\partial\xi}\\ + \alpha\left\{\left(\frac{K_{xy}}{D}+\frac{K_{yx}}{D}\right)\left(\frac{\partial^2\theta}{\partial\xi\partial Y} - \frac{Y}{3\xi}\frac{\partial^2\theta}{\partial Y^2} - \frac{1}{3\xi}\frac{\partial\theta}{\partial Y}\right)\right.\\ \left. + \frac{\partial(K_{yx}/D)}{\partial Y}\left(\frac{\partial\theta}{\partial\xi} - \frac{Y}{3\xi}\frac{\partial\theta}{\partial Y}\right)\right\}\\ - \alpha^2\left\{\frac{\partial^2\theta}{\partial\xi^2} - \frac{2Y}{3\xi}\frac{\partial^2\theta}{\partial\xi\partial Y} + \frac{Y^2}{9\xi^2}\frac{\partial^2\theta}{\partial Y^2} + \frac{5}{9}\frac{Y}{\xi^2}\frac{\partial\theta}{\partial Y}\right\}\\ \times\left(1+\frac{K_{xx}}{D}\right) = 0.\end{aligned} \tag{25}$$

For a long plate, $\alpha = \sqrt[3]{9X}/L \ll 1$, and the analysis may therefore be restricted to the α-zero approximation

$$\left(1+\frac{9b}{\sqrt{Pr}}XY^3\right)\frac{\partial^2\theta}{\partial Y^2} + 3Y^2\left(1+\frac{9b}{\sqrt{Pr}}X\right)\frac{\partial\theta}{\partial Y} - 9XY\frac{\partial\theta}{\partial X} = 0, \tag{26}$$

$$\theta(-\infty, Y) = 0;\quad \theta(X,\infty) = 0;$$

$$\frac{\partial\theta}{\partial Y}(X,0) = \begin{cases} K\sqrt[3]{9X}[\theta(X,0)-1] & \text{at } 0 < X < L \\ 0 & \text{at } X < 0, X > L. \end{cases} \tag{27}$$

It is quite obvious that equation (26) includes only one tensor component of the eddy diffusivity K_{yy} which can be estimated with an appropriate accuracy [22]. Things are more intricate with other components K_{xx}, K_{xy} and K_{yx}, no information being available in literature on their behaviour in the viscous sublayer of the turbulent boundary layer.

With regard for equation (26), the limit laws of the local mass transfer intensity on the plate are easily obtained for short and long distances from the leading edge of the plate.

In the first case discussed in detail above, the effect of turbulent mass transfer can be neglected. According to formulae (12), (16), (18) and (21) at finite k

$$\begin{aligned}Nu &= \frac{kl}{D}\left[1 - \frac{\sqrt[3]{9}}{\Gamma(2/3)}KX^{1/3} + \ldots\right]\\ &= \frac{kl}{D}\left[1 - \frac{\sqrt[3]{9}}{\Gamma(2/3)}Pr^{2/3}\frac{k}{u_*}x_+^{1/3} + \ldots\right]\end{aligned} \tag{28}$$

and

$$Nu = \frac{\sqrt[3]{3}}{\Gamma(1/3)}\frac{L}{X^{1/3}} = \frac{\sqrt[3]{3}}{\Gamma(1/3)}\frac{l_+}{x_+^{1/3}}Pr^{1/3} \tag{29}$$

at $k = \infty$.

For $X \gg 1$, when the concentration field close to the plate varies slightly along x, equation (26) assumes the form

$$\frac{\partial}{\partial Y}\left[\left(1+\frac{9b}{\sqrt{Pr}}XY^3\right)\frac{\partial\theta}{\partial Y}\right] = 0. \tag{30}$$

Its solution at boundary conditions (27) has the form

$$\theta = \frac{1}{1+\dfrac{3\sqrt{3}}{2\pi}\dfrac{\sqrt[3]{b}}{G}}\left[1 - \frac{3\sqrt{3}}{2\pi}\int_0^{\sqrt[3]{b}\sqrt{Pr}\,y_+}\frac{du}{1+u^3}\right] \tag{31}$$

Hence, for the flow region analyzed, we obtain at finite k

$$Nu_\infty = \frac{\dfrac{3\sqrt{3}}{2\pi}\sqrt[3]{b}\,l_+\,Pr^{1/3}}{1+\dfrac{3\sqrt{3}}{2\pi}\dfrac{\sqrt[3]{b}}{G}} \tag{32}$$

and at $k = \infty$

$$Nu_\infty = \frac{3\sqrt{3}}{2\pi}\sqrt[3]{b}\,l_+\,Pr^{1/3}. \tag{33}$$

To solve equation (26) at any x, the approximate moment method [23, 24] is used. This method has been successfully applied for deriving integral momentum and energy relationships (see, for example [25]). Require that equation (26) be "on the average" satisfied. With this end in view, rewrite equation (26) of the α-zero approximation and boundary conditions (27) as follows

$$y_+\frac{\partial\theta}{\partial x_+} = \frac{\partial}{\partial y_+}\left[\left(\frac{1}{Pr}+by_+^3\right)\frac{\partial\theta}{\partial y_+}\right], \tag{34}$$

$$\theta(x_+,\infty) = 0;\quad \frac{\partial\theta}{\partial y_+}(x_+,0) = \frac{k}{u_*}Pr[\theta(x_+,0)-1]. \tag{35}$$

After substituting the variable $z = y_+/\delta(x_+)$ assume that dimensionless concentration profiles of passive admixture may, with sufficient accuracy, be considered affine-similar in z [23, 24]. Then an ordinary differential equation of the first order with respect to the boundary-layer thickness $\delta(x_+)$ and of the second order with respect to $\theta(z)$ is of the form

$$z^2\frac{\theta'}{\theta''}Pr\delta^2\delta' + \left(3z^2\frac{\theta'}{\theta''} + z^3\right)bPr\delta^3 + 1 = 0 \tag{36}$$

with the boundary conditions

$$\theta(\infty) = 0,\ \theta'(0) = \delta\frac{k}{u_*}Pr[\theta(0) - 1] \tag{37}$$

$$\delta(0) = 0 \quad \text{at} \quad k \to \infty. \tag{38}$$

Here the point and prime mean differentiation in x_+ and z, respectively. On integrating equation (36) from 0 to 1 and setting the expression obtained equal to zero, we arrive at the equation

$$\gamma Pr\delta^2\delta' + \beta bPr\delta^3 + 1 = 0 \tag{39}$$

where

$$\gamma = -\int_0^1 \xi^2\frac{\theta'(\xi)}{\theta''(\xi)}\,d\xi,\ \beta = -3\int_0^1 \xi^2\frac{\theta'(\xi)}{\theta''(\xi)}\,d\xi - \tfrac{1}{4}. \tag{40}$$

Equation (39) is an approximate correlation replacing original equation (26). Naturally, the agreement between the below results and accurate correlations is controlled by the parameters γ and β, i.e. by the proper choice of the function $\theta(z)$. The previous formulae, being asymptotically correct, can be of use here. Indeed, the comparison of the relevant asymptotic expansions of the approximate solution with the accurate formulae permits not only the required relationships between the constants γ and β to be obtained, but also the choice of $\theta(z)$ to be estimated. Thus, we can get an idea on the accuracy of the approximate solution and, thereby, eliminate, to a certain extent, the most essential imperfection of the approximate methods.

The solution of differential equation (39) takes the form

$$\int_{\sqrt[3]{\beta bPr\delta(0)}}^{\sqrt[3]{\beta bPr\delta(x_+)}} \frac{u^2\,du}{1-u^3} = \frac{\beta}{\gamma}bx_+. \tag{41}$$

It is easy to see that in our notations

$$\sqrt[3]{\beta bPr}\,\delta(x_+) = Nu_\infty/Nu(x_+). \tag{42}$$

By using equations (28), (32) and (41), one can find

$$\int_B^{Nu_x/Nu_\infty} \frac{u^2\,du}{1-u^3} = \frac{\beta}{\gamma}bx_+,\ B^{-1} = 1 + \frac{2\pi}{3\sqrt{3}}\frac{G}{\sqrt[3]{b}}. \tag{43}$$

The upper limit of the integral tends to zero at $k \to \infty$, i.e. $\delta(0) \to 0$ in accordance with equation (29), but at a finite k the thickness of the diffusional boundary layer at the leading edge differs from zero by virtue of boundary condition (37).

At $k \to \infty$ and $bx_+ \ll 1$, one can see from equations (33) and (43) that

$$Nu = \frac{3\sqrt{3}}{2\pi}\sqrt[3]{\frac{\gamma}{3\beta}}\frac{l_+}{x_+^{1/3}}Pr^{1/3}. \tag{44}$$

Then the ratio β/γ can be estimated by comparing the above result with asymptotically correct equation (29)

$$\frac{\beta}{\gamma} = \left[\frac{3\sqrt{3}}{2\pi}\frac{\Gamma(1/3)}{\sqrt[3]{9}}\right]^3 = \frac{3}{\Gamma^3(2/3)}. \tag{45}$$

The function describing the distribution of the dimensionless local mass-transfer intensity can now be expressed as

$$Nu = \frac{Bkl/D}{\sqrt[3]{1-(1-B^3)\exp[-9\Gamma^{-3}(2/3)bx_+]}}. \tag{46}$$

All of the above reasonings are also valid for heat and mass transfer in tubes and channels of an arbitrary cross section, l being the tube diameter or the equivalent rectilinear channel diameter. The above correlations allow calculation of heat and mass transfer in the entry region of the channels both for $Pr \gg 1$ and for a stabilized velocity profile. At a great distance from the entrance, the dimensionless mass-transfer intensity is stabilized and can be calculated by formula (32) which becomes equation (33) at $k = \infty$.

It should be noted here that in accordance with formula (32) the stabilized Nu number at a finite rate of the wall reaction may considerably differ from Nu_∞ at $k \to \infty$. This may partially account for the difference in Nu_∞ numbers obtained in some electrochemical experiments [26, 27] and in the experiments dealing with dissolution of the inner tube surface [28 31]. This point of view is to some extent supported by the Canadian scientists [32, 33]. These authors have paid much attention to the surface cleanness of the electrochemical sensors and have almost eliminated the above divergence. Also in Fig. 4 of [26] one can observe an existing difference (increasing with Re number) between the experimental data and theoretical relation (29) obtained at $k = \infty$. The partial blocking of the electrochemical sensor surfaces is believed to require introduction of the "effective rate" of the electrochemical reaction to allow for this blocking in appropriate calculations.

The function describing the relative increase of heat and mass transfer in the entry region can be easily obtained from formulae (46) and (32) as

$$\frac{Nu}{Nu_\infty} = \frac{1}{\sqrt[3]{1-(1-B^3)\exp[-9\Gamma^{-3}(2/3)bx_+]}}. \tag{47}$$

Table 2

Reference	$Re \times 10^{-3}$	G	Nu $k =$	calc. $k = 0.09$ cm/s	Nu_{exp}
26	75	0.91	4070	3720	3150
27	50	0.20	2840	1970	2150
	30	0.32	1770	1410	1400
	20	0.46	1245	1050	1000
	10	0.83	690	625	550

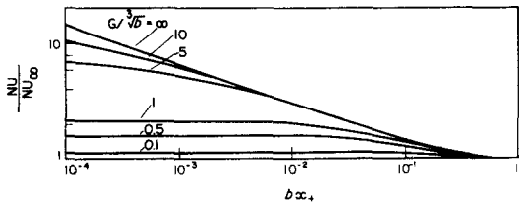

FIG. 5. Nomogram of $Nu/Nu_\infty = f(G/\sqrt[3]{b},\ bx_+)$. [Calculated by formula (47).]

The nomogram for the results of calculation according to this formula is given in Fig. 5. It is seen that at $G \gtrsim 10\sqrt[3]{b}$ the desired ratio is satisfactorily approximated by the formula obtained from equation (47) at $G \to \infty$

$$\frac{Nu}{Nu_\infty} = \frac{1}{\sqrt[3]{1-\exp(-3.62bx_+)}}. \quad (48)$$

This formula is more simple than the equation suggested in [34] and better fits the detailed analytical solution derived there; the deviation does not exceed 1%.

At a finite G in the vicinity of the leading edge, the correlation

$$\frac{Nu}{Nu_\infty} = \frac{1+1.21G/\sqrt[3]{b}}{\sqrt[3]{1+3.62(B^{-3}-1)bx_+}} \text{ at } bx_+ \ll 1/4 \quad (49)$$

is valid.

Therefore, the curves for Nu/Nu_∞ in logarithmic coordinates approach, at $bx_+ \to 0$, the following asymptote (which is more noticeable at small G)

$$Nu/Nu_\infty = 1+1.21G/\sqrt[3]{b} \text{ at } bx_+ \ll 1/4. \quad (50)$$

The stabilization length of the local mass-transfer intensity depends on the chosen accuracy of $r_*\% = r_*/100$. It is clear, however, that at a rather small G, it is pointless to discuss the stabilization length of local mass transfer, since in the range of the chosen accuracy the ratio Nu/Nu_∞ can be considered constant over the whole length. At $G \to \infty$, the unknown length is estimated from the equation

$$bl_{s+} = 1+0.28\ln(1/r_*). \quad (51)$$

The correlation obtained from formula (47) to describe the relative increase of the sensor length-averaged mass-transfer intensity is of the form

$$\frac{\langle Nu\rangle}{Nu_\infty} = \frac{1}{1.21bl_+}\left\{\frac{1}{6}\ln\left[\frac{1+u+u^2}{1+B+B^2}\frac{(1-B)^2}{(1-u)^2}\right] - \frac{1}{\sqrt{3}}\left(\arctan\frac{1+2u}{\sqrt{3}} - \arctan\frac{1+2B}{\sqrt{3}}\right)\right\} \quad (52)$$

where

$$u = \sqrt[3]{1-(1-B^3)\exp(-3.62bl_+)}.$$

The results found by this formula are presented in Fig. 6. It is clear from Fig. 6 that at finite G, the above ratio in logarithmic coordinates approaches the asymptote $\langle Nu\rangle/Nu_\infty = 1+1.21G/\sqrt[3]{b}$ that, naturally, coincides with the asymptote of Nu/Nu_∞.

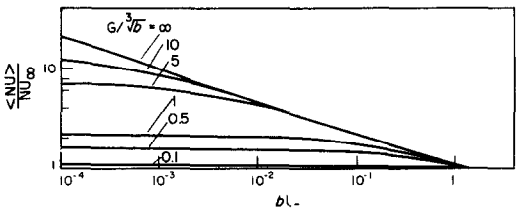

FIG. 6. Nomogram of $\langle Nu\rangle/Nu_\infty = f(G/\sqrt[3]{b},\ bl_+)$. [Calculated by (52).]

Just as in the case of the local mass-transfer intensity, it can be assumed that at rather small G, relation (52) remains constant along the film sensor within the chosen accuracy and hence it is no sense in discussing the length necessary for $\langle Nu\rangle$ stabilization. For greater values of the parameter G, however, the problem is of considerable interest and the unknown length may be estimated by the formula

$$bL_{s+} = 20(1-B^3)/r_*. \quad (53)$$

Without loss of accuracy, one can use the approximate equation

$$\frac{\langle Nu\rangle}{Nu_\infty} = \frac{1}{\sqrt[3]{1-(1-B^3)\exp\left[-\frac{8}{3}\Gamma^{-3}(2/3)bl_+\right]}} \quad (54)$$

instead of more complicated equation (52).

The comparison (see Fig. 7) of the predictions performed by formula (52) (in assumption that $G = \infty$ and $b = 10^{-3}$) with the experimental data [28–30] on dissolution of the inner tube surface shows that the available data do not contradict the theory. A significant scatter of the experimental data does not allow a more definite conclusion. Note that in some of the

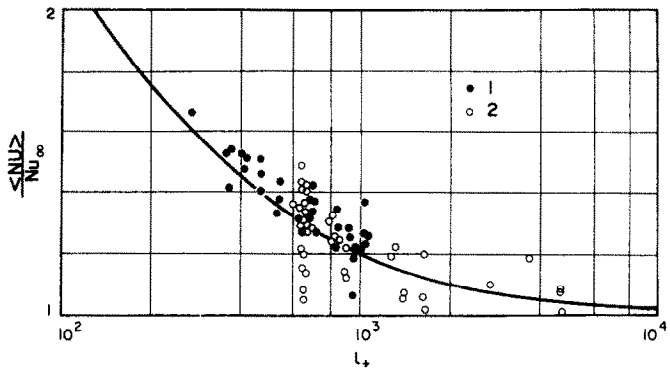

FIG. 7. Comparison of calculations by (52) with experimental data for $G = \infty$. 1, [28]; 2, [29, 30].

experimental data [29, 30] obtained at $Re = 10^4$ ($l_+ = 610$–650) and covering a range of the Prandtl numbers between 930 and 97 000, the ratio $\langle Nu \rangle / Nu_\infty$ tends to decrease slightly with the increase of Pr. This tendency cannot be explained by the above theory that predicts the relation $\langle Nu \rangle / Nu_\infty = \text{constant}$ at $l_+ = \text{constant}$ independent of Pr and is completely inconsistent with the theory that uses an assumption on the proportionality of the eddy diffusivity within the viscous sublayer to the fourth power of the distance from the wall. According to this theory, the ratio $\langle Nu \rangle / Nu$, should also increase with Pr at constant l_+.

The comparison of the results of the developed theory with the only known to us experimental work [27] describing the experimental electrochemical investigation of local mass-transfer intensity in the mass-transfer entry region is difficult for two reasons. The one is that the author of [27], assuming for the local mass-transfer coefficient the value averaged over the sensors of finite width (1, 2 and 3 mm), related it to the distance x from the start of the mass-transfer entry region to the central point of the sensor. This leads to greater values of the mass-transfer coefficients in the region of large mass flux gradients which are characteristic of small x's. The recalculation of the experimental data (being quite possible in the framework of the developed theory) is, however, deprived of any meaning due to the second factor which is difficult to be taken into account. This is the influence of packings that insulate the local mass-transfer sensor from the rest portion of the tube. Despite their small (in absolute measurements) thickness (~ 0.1 mm) they can essentially damage the diffusion boundary layer, which is very thin in these conditions, and lead to noticeable errors of the same sign in the mass flux quantities.

The comparison between the predictions for $k = 5 \times 10^{-4}$ m/s, $b = 0.5 \times 10^{-3}$ and the experimental electrochemical data on the averaged rates of turbulent transfer to a tube wall in the mass-transfer entry region [26] is presented in Fig. 8. Quite satisfactory agreement between theory and experiment is readily seen there. The value of $k = 5 \times 10^{-4}$ m/s, used in the calculation, has been found in the following way. On a small ring the diffusional boundary layer is so thin that

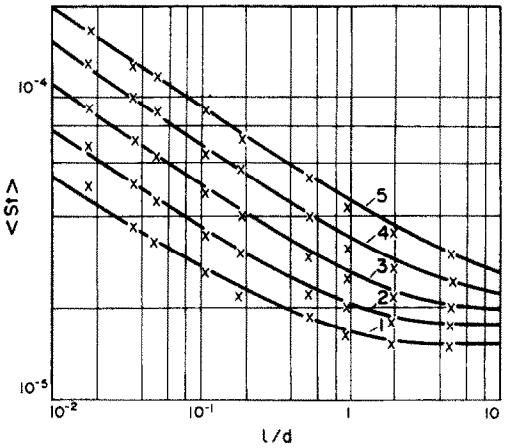

FIG. 8. Comparison of theoretical calculations with experimental data [26] for length-averaged rates of turbulent transfer in the mass transfer entry region ($Pr = 2400$, $k = 0.5 \times 10^{-3}$ m/s, $b = 0.5 \times 10^{-3}$).

Nos.	1	2	3	4	5
$Re \times 10^{-3}$	75	40	20	10	5

the turbulent diffusion is negligible and mass transfer can be calculated with the aid of equation (54) which may be rewritten in the form

$$\langle St \rangle \left(\frac{l}{d}\right)^{1/3} = \frac{\langle Nu \rangle}{RePr}\left(\frac{l}{d}\right)^{1/3} = \frac{3.68 \times 10^{-4}\sqrt{\lambda/8}\sqrt[3]{l/d}}{\sqrt[3]{B^3 + 0.54 \cdot 10^{-3} l_+}}$$

$$B = 1/(1 + 2740k/u_*), \quad l_+ = (l/d)Re\sqrt{\lambda/8}. \tag{55}$$

At $k \to \infty$ it must be

$$\langle St \rangle \left(\frac{l}{d}\right)^{1/3} = \frac{1.54 \times 10^{-3}}{Re^{5/12}}. \tag{56}$$

Comparison between the above formulae and the experimental data gives the value of k.

Solid line 2 is plotted in Fig. 9, borrowed from [26], for formula (55) at $k = 5 \times 10^{-4}$ m/s and $l/d = 0.1$. One can see that the above theory explains the existing difference between the experimental results and theoretical calculations assuming $k = \infty$ [see formula (56)].

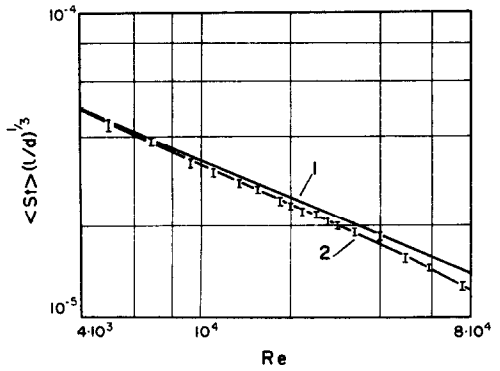

FIG. 9. Comparison of mass-transfer data [26] for small rings with equations (55), (56). 1: calculated by formula (56) at $k = \infty$; 2: calculated by formula (55) at $k = 5 \times 10^{-4}$ m/s; vertical bars denote the range of experimental data.

REFERENCES

1. P. Grassman, N. Ibl an J. Trüb, Electrochemische Messung on Stoffübergangszahlen, *Chemie Ingr Tech.* **33**, 529 533 (1961).
2. O. Hoffer, Über die Entwicklung einer Heissfoliensonde für Messungen in turbulenten Strömungen, *Arch. tech. Messen.* No. 444, 5–10 (1973).
3. L. P. Reiss and T. J. Hanratty, Measurement of instantaneous rates of mass transfer to a small sink on a wall, *A.I.Ch.E. Jl* **8**, 245–247 (1962).
4. S. C. Ling, Heat transfer from a small isothermal spanwise strip on an insulated boundary, *J. Heat Transfer* **85**, 230–236 (1963).
5. J. E. Mitchell and T. J. Hanratty, A study of turbulence at a wall using an electrochemical wall shear-stress meter, *J. Fluid Mech.* **26**, 199–211 (1966).
6. K. K. Sirkar and T. J. Hanratty, Limiting behaviour of the transverse turbulent velocity fluctuations close to a wall, *I/EC Fundamentals* **8**, 189–192 (1969).
7. G. Fortuna and T. J. Hanratty, Frequency response of the boundary layer on a wall transfer probe, *Int. J. Heat Mass Transfer* **14**. 1499–1507 (1971).
8. B. M. Smolsky and V. P. Popov, Mass transfer problem for electro-chemical diffusional converters of mechanical quantities, in *Collected papers "Problems of Heat and Mass Transfer"*, pp. 123–136. Energiya, Moscow (1970).
9. Yu. E. Bogolyubov, P. I. Geshev, V. E. Nakoryakov and I. A. Ogorodnikov, Theory of electrodiffusional method of measuring spectral characteristics of turbulent flows, *Zh. Prikl. Mekh. Tekh. Fiz.* **4**, 113–121 (1972).
10. V. E. Nakoryakov, A. P. Burdukov, B. G. Pokusaev, V. A. Kuzmin, V. A. Utkovich, V. V. Khristoforov and Yu. V. Tatevosyan, *Turbulent Two-Phase Flows.* Izd. Inst. Teplofiz. Sib. Otd. AN SSSR, Novosibirsk (1973).
11. M. Lebouche, Relation entre les fluctuations parietales du transfer massique et du gradient de vitèsse dans le gas d'un nombre de Schmidt grand, *CR. He d. Séanc. Acad. Sci., Paris* **271A**, 438–441 (1970).
12. H. Matsuda, Zur Theorie der Elektrolyse mit zwei eng benachbarten Elektroden in Strömungsanordnungen. Allgemeine Formel für die Übertragungsausbeute, *J. Electroanal. Chem.* **16**, 153–164 (1968).
13. T. Mizushina, H. Yeda and T. Maruyama, Dynamic behaviour of transfer coefficients, in *Collected papers "Heat and Mass Transfer"*, Izd. ITMO AN BSSR 1, part 3,10. Minsk (1972).
14. A. Acrivos and P. L. Chambrè, Laminar boundary layer flows with surface reactions, *Ind. Engng Chem.* **49**, 1025–1029 (1957).
15. D. A. Frank-Kamenetsky, *Diffusion and Heat Transfer in Chemical Kinetics.* Nauka. Moscow (1967).
16. M. A. Leveque, Transmission de chaleur par convection, *Anns Mines Carbur., Paris* **13**. 12 (1928).
17. S. G. Springer and T. J. Pedley, The solution of heat transfer problems by the Wiener–Hopf technique. I. Leading edge of a hot film, *Proc. R. Soc.* **A333**(1594), 347–362 (1973).
18. D. A. Popov, Problem with discontinuous boundary conditions and diffusional boundary-layer approximation, *Prikl. Mat. Mekh.* **39**(1), 109–117 (1975).
19. B. A. Kader, Structure of the concentration field at the leading edge of the diffusional sensor, *Elektrokhimiya* **13**, 488–496 (1977).
20. J. Boussinesq, Essai sur la théorie des eaux courants, *Mém. Près. Div. Sav. Acad. Sci. Inst. Fr.* **23**, 1–680 (1877).
21. A. M. Yaglom, Horizontal turbulent transport of heat in the atmosphere and the form of the eddy diffusivity tensor, *Fluid Dynam. Trans.* **4**, 801–812 (1962).
22. B. A. Kader and A. R. Aronov, The statistical analysis of the experimental works of heat and mass transfer at high *Pr* numbers. *Teor. Osnovy Khim. Tekhnol.* **4**, 637 652 (1970).
23. B. A. Finlayson, Application of the method of weighted residuals and variational methods, *Br. Chem. Engng* **14**, 53–57 (1969).
24. B. A. Finlayson, Application of the method of weighted residuals and variational methods, *Br. Chem. Engng* **14**, 179–182 (1969).
25. H. Schlichting, *Grenzschicht-Theorie.* G. Braun, Karlsruhe (1965).
26. P. Show, L. P. Reiss and T. J. Hanratty, Rates of turbulent transfer to a pipe wall in the mass transfer entry region, *A.I.Ch.E. Jl* **9**(3), 362–364 (1963).
27. G. Schütz, Untersuchung des Stoffaustauschanlaufgebietes in einem Rohr bei vollausgebildeter hydrodynamischer Strömung mit einer electrochemischen methode, *Int. J. H at Mass Transfer* **10**, 1077 1082 (1964).
28. E. S. C. Meyerink and S. K. Friedlander, Diffusion and diffusion controlled reactions in fully developed turbulent pipe flow, *Chem. Engng Sci.* **17**, 121–135 (1962).
29. R. M. Hamilton, Solid–liquid mass transfer in turbulent pipe flow, Ph.D. Thesis, Cornell Univ. (1963).
30. P. Harriott and R. M. Hamilton, Solid–liquid mass transfer in turbulent pipe flow, *Chem. Engng Sci.* **20**, 1073–1078 (1965).
31. A. A. Gukhman and B. A. Kader, Solid–liquid mass transfer in turbulent pipe flow at high Schmidt numbers, *Teor. Osnovy Khim. Tekh.* **3**, 216–224 (1969).
32. D. A. Dawson, High Schmidt number mass transfer near rough surfaces, Ph.D. Thesis, Univ. Toronto (1968).
33. D. A. Dawson and O. Trass, Mass transfer at rough surfaces, *Int. J. Heat Mass Transfer* **15**, 1317–1336 (1972).
34. B. A. Kader and V. V. Dilman, Heat and mass transfer in the entry region of turbulent flow at $Pr \gg 1$, *Teor. Osnovy Khim. Tekh.* **7**, 210–222 (1973).

TRANSFERT MASSIQUE TURBULENT AVEC UNE REACTION CHIMIQUE DU PREMIER ORDRE SUR UNE PAROI A $Pr \gg 1$

Résumé—On étudie le transfert massique entre un écoulement turbulent et une paroi plane et lisse sur laquelle se développe une réaction chimique du premier ordre. On analyse le cas extrême d'une vitesse de réaction infiniment élevée (concentration constante de mélange passif sur la paroi). On considère successivement trois cas possibles. Pour les plaques très courtes qui ne peuvent être décrites par

l'approximation de couche limite, une solution est obtenue sur ordinateur par la méthode aux différences finies. Cette solution couvre complètement les effets de bord (diffusion meléculaire longitudinale d'un mélange passif) et de surface (réaction chimique à vitesse finie) qui sont essentiels pour les plaques de petite longueur. Pour les plaques qui peuvent être étudiées par l'approximation de la couche limite en négligeant l'effet du transfert massique turbulent, la solution analytique est obtenue. Les résultats numériques sont comparés avec ceux obtenus par la méthode de la surface également accessible et par l'approximation de couche limite. La limite inférieure de la dimension de plaque est atteinte quand les effets de bord peuvent être négligés. Ces résultats sont directement applicables à la théorie des détecteurs à film de petite dimension, à électrodiffusion ou thermique (avec revêtement), mais aussi à la conception des mesures locales de frottement, de transfert de chaleur et de masse entre une surface lisse et un fluide.

TURBULENTER STOFFÜBERGANG MIT EINER CHEMISCHEN REAKTION ERSTER ORDNUNG AN EINER WAND BEI $Pr \gg 1$

Zusammenfassung—Der Stoffübergang zwischen einer turbulenten Strömung und einer ebenen glatten Wand mit einer chemischen Reaktion erster Ordnung an deren Oberfläche wurde untersucht. Ein Extremfall einer unendlich hohen Reaktionsrate (konstante Konzentration passiver Beimischung an der Wand) wurde analysiert. Drei mögliche Fälle werden nacheinander betrachtet. Für sehr kurze Platten, die nicht mit der Grenzschichtnäherung beschrieben werden können, wurde eine Lösung mit einem Rechenprogramm nach der Methode finiter Differenzen gefunden. Diese Lösung mit einem Rechenprogramm nach der Methode finiter Differenzen gefunden. Diese Lösung läßt Effekte zu, die für kurze Platten ziemlich wesentlich sind und zwar sowohl für den Rand (longitudinale, molekulare Diffusion eines passiven Zusatzes) als auch für die Oberfläche (endliche Umsatzrate einer chemischen Reaktion). Für solche Platten, die mit der Grenzschichtnäherung unter Vernachlässigung der Wirkung des turbulenten Stoffübergangs gedeckt werden können, ist die analytische Lösung der Aufgabe abgeleitet worden. Die numerischen Daten werden mit denen verglichen, die nach der Methode der gleichmässig zugänglichen Oberfläche und nach der Grenzschichtnäherung gewonnen wurden. Als Ergebnis kann die untere Grenze der Plattengröße, bei der die Randeinflüsse vernachlässigt werden dürfen, festgelegt werden. Diese Ergebnisse können unmittelbar auf die Theorie der Elektrodiffusions-Miniatursensoren und der thermischen Miniatursensoren (mit Beschichtung) und dem Mikrofilmprinzip angewendet werden. Diese Sensoren werden dazu verwendet, um örtliche Werte der Reibung und des Wärme- und Stoffübergangs an eine glatte, feste Wand in einem Fluid zu messen.

ТУРБУЛЕНТНЫЙ МАССОПЕРЕНОС С ХИМИЧЕСКОЙ РЕАКЦИЕЙ ПЕРВОГО ПОРЯДКА НА СТЕНКЕ ПРИ $Pr \gg 1$

Аннотация — Рассматривается массоперенос между турбулентным потоком жидкости и плоской гладкой стенкой, на поверхности которой происходит химическая реакция первого порядка. Анализируется также предельный случай бесконечно большой скорости реакции, когда концентрация пассивной примеси на стенке принимает постоянное значение.

Последовательно разбираются три возможных случая. Для очень коротких пластин в условиях, когда приближение пограничного слоя неприменимо, с помощью ЭВМ конечно-разностным способом получено решение, в котором в полной мере учитываются как краевые (продольная молекулярная диффузия пассивной примеси), так и поверхностные эффекты (конечная скорость химической реакции), весьма существенные для пластин малой длины. Для коротких пластин, когда допустимо использовать приближение пограничного слоя и, одновременно, пренебречь вкладом турбулентного механизма переноса, получено аналитическое решение задачи. Данные численных расчетов сравниваются с результатами анализа, проведенного в приближении пограничного слоя и методом равнодоступной поверхности. На основе такого сравнения удается установить нижнюю границу области размеров пластин, в которой допустимо пренебрегать влиянием краевых эффектов. Эти результаты могут быть непосредственно использованы в теории электродиффузионных и тепловых (с покрытием) пленочных датчиков весьма малых размеров, предназначенных для измерения локальных характеристик трения, тепло- и массопереноса на твердую гладкую стенку, омываемую потоком жидкости.

В случае длинных пластин, для которых существенную роль играет турбулентный механизм массопереноса, получено простое приближенное решение задачи. Числовые значения параметров, входящих в это решение, выбирались таким образом, чтобы они совпали с полученными ранее точными асимптотическими результатами вблизи передней кромки пластины и вдали от нее. Полученные результаты позволяют, в частности, определить длину начального участка канала произвольного сечения, необходимую для стабилизации массопереноса, и предложить простые формулы для расчета локальной и осредненой по длине канала интенсивности массообмена на начальном участке. Эти формулы сравниваются с имеющимися в литературе опытными данными.